Journal of the Chinese Institute of Engineers, Vol. 22, No. 6, pp. 785-793 (1999)

APPROXIMATE DYNAMIC CRACK FRICTIONAL CONTACT ANALYSIS FOR 3D STRUCTURE

P. H. Wen* and M. H. Aliabadi
Department of Engineering
Queen Mary and Westfield College, London University
London E1 4NS, UK

A. Young
Structural Materials Centre
DERA, Farnborough
Hants, GU14 6TD, UK

Key Words: boundary element method, contact mechanics, fracture mechanics, dynamic stress intensity factors.

ABSTRACT

In this paper the dual boundary element formulation is developed to study crack surface contact problem with friction dynamic loads. The nonlinear three-dimensional dynamic problem can be treated as linear problem by three assumptions. The dual boundary integral equations are given in the Laplace transform domain with the boundary varibles of displacement and traction on the external boundary and displacement discontinuities on the crack surface. Durbin's Laplace tranfrom inversion method is used and the dynamic stress intensity factors are determined by crack opening displacement. A rectangular bar containing a slant circular crack under a pressure Heaviside load is studied. The influrence of different elasticity waves on the dynamic stress intensity factors $K_{II}(t)$ and $K_{III}(t)$ are analysed in detail.

I. INTRODUCTION

Contact problem research in many areas is very important for engineering design. In solid static research, Hertz, in 1882, obtained analytical solutions for the contact pressure and the indentation for elastic bodies with quadratic surfaces without friction. In general, the contact region and contact pressure depend on the external load, the elasticity properties and the friction between contact bodies. Such dependence makes the contact problem nonlinear and as such the only possible way to solve this problem is to use numerical methods such as the finite element method (see Wilson and Parson, 1970 and Chan and Tuba, 1971). The boundary element method (BEM) has also increasingly been used. As the contact is on the boundary, BEM would be more suitable to the analysis of contact problem, see for example by Andersson (1983) and Man, *et al.* (1993). Traction boundary integral equations were deduced by Hong and Chen (1988) and applied to crack problems with high accuracy. Comprehensive review can be found in paper by Chen and Hong (1999).

There is particular type of contact in fracture mechanics. The two crack surfaces contact can occur under the external load. For instance, if the stress intensity factor K_I is less than zero, the contact

*Correspondence addressee

occurs at least in front of the crack tip. By use of the displacement discontinuity method, Wen and Wang (1991) studied an arc crack under uniaxial tension and pressure and obtained the real stress intensity factors with consideration of frictional contact between two crack surfaces. An approximate analysis of dynamic contact between crack surfaces without friction for two dimensional problem was introduced by Wen, *et al.* (1995) using indirect boundary element method with successive approximation.

In this paper we study three dimensional flat crack contact problems using the dual boundary element method which was developed for three dimenisonal elastostatic problems by Mi and Aliabadi in 1992. Because the embedded crack is flat in the body, the contact region and the direction of friction are assumed to be known. With two assumptions, the nonlinear dynamic problem can be transformed to a linear problem. Boundary integral equations, with external boundary condition and crack contact condition, are given in the Laplace transform domain. The unknown boundary values (traction or displacement) on external boundary and displacement discontinuities and contact pressure on the crack surface can be determined numerically. Dynamic stress intensity factors K_{II} and K_{III} in the time domain are obtained by use of the Durbin's Laplace transform inversion method (1974). Numerical calculations have been carried out for a square bar containing a slant circular crack under dynamic uniform load at the top. The influence of elasticity waves on stress intensity factors can be seen clearly from these results.

II. DUAL BOUNDARY ELEMENT METHOD IN LAPLACE TRANSFORM DOMAIN

Consider a cracked isotropic elastic body Ω enclosed by an outer boundary Γ_e. The body containing a crack, boundary Γ_c, is subjected to a dynamic load on the external boundary.

The Navier–Cauchy equation in the time domain is given in Balas *et al.* (1989), for zero body force, by

$$c_2^2 u_{i,kk} + (c_1^2 - c_2^2) u_{k,ki} = \frac{\partial^2 u_i}{\partial t^2}, \quad i=1, 2, 3, \tag{1}$$

where c_1 and c_2 are the velocities of dilatation and shear waves respectively. Taking Laplace transforms, Eq. (1) becomes

$$c_2^2 \tilde{u}_{i,kk} + (c_1^2 - c_2^2) \tilde{u}_{k,ki} = s^2 \tilde{u}_i \tag{2}$$

where the initial (t=0) displacements and velocities are assumed to be zero. The Laplace transform of a function $f(\boldsymbol{x}, t)$ is defined as

$$\mathcal{L}[f(\boldsymbol{x}, t)] = \tilde{f}(\boldsymbol{x}, s) = \int_0^\infty f(\boldsymbol{x}, t) e^{-st} dt \tag{3}$$

where s is Laplace transform parameter. In the transform domain, the solution of (2) should satisfy the boundary conditions, i.e.

$$\tilde{u}_i(\boldsymbol{x}, s) = \tilde{u}_i^0(\boldsymbol{x}, s) \tag{4}$$

on displacement boundary and

$$\tilde{t}_i(\boldsymbol{x}, s) = \tilde{t}_i^0(\boldsymbol{x}, s) \tag{5}$$

on traction boundary, where $\tilde{u}_i^0(\boldsymbol{x}, s)$ and $\tilde{t}_i^0(\boldsymbol{x}, s)$ respectively denote transformed displacement and traction boundary conditions.

The displacement at a point $\boldsymbol{X}'$ in the domain Ω (called a collocation point) can be determined from the boundary values of displacement and traction through the Somigliana's identity. If the tractions on a flat crack surfaces are equilibrium, i.e. $\tilde{t}_j^+(\boldsymbol{x}) = -\tilde{t}_j^-(\boldsymbol{x}) = \tilde{t}_j(\boldsymbol{x})$, we have

$$\begin{aligned}\tilde{u}_i(\boldsymbol{X}', s) = &\int_{\Gamma_e} \tilde{U}_{ij}(\boldsymbol{X}', \boldsymbol{x}, s) \tilde{t}_j(\boldsymbol{x}) d\Gamma(\boldsymbol{x}) \\ &- \int_{\Gamma_e} \tilde{T}_{ij}(\boldsymbol{X}', \boldsymbol{x}, s) \tilde{u}_j(\boldsymbol{x}) d\Gamma(\boldsymbol{x}) \\ &- \int_{\Gamma_c} \tilde{T}_{ij}(\boldsymbol{X}', \boldsymbol{x}, s) \Delta\tilde{u}_j(\boldsymbol{x}) d\Gamma(\boldsymbol{x}) \\ &i, j=1, 2, 3\end{aligned} \tag{6}$$

By use of Hooke's law, the stress components at point $\boldsymbol{X}'$ can be expressed as following:

$$\begin{aligned}\tilde{\sigma}_{ij}(\boldsymbol{X}', s) = &\int_{\Gamma_e} \tilde{U}_{kij}(\boldsymbol{X}', \boldsymbol{x}, s) \tilde{t}_k(\boldsymbol{x}) d\Gamma(\boldsymbol{x}) \\ &- \int_{\Gamma_e} \tilde{T}_{kij}(\boldsymbol{X}', \boldsymbol{x}, s) \tilde{u}_k(\boldsymbol{x}) d\Gamma(\boldsymbol{x}) \\ &- \int_{\Gamma_c} \tilde{T}_{kij}(\boldsymbol{X}', \boldsymbol{x}, s) \Delta\tilde{u}_k(\boldsymbol{x}) d\Gamma(\boldsymbol{x}) \\ &i, j=1, 2, 3\end{aligned} \tag{7}$$

where $\Delta\tilde{u}_k(\boldsymbol{x}) = \tilde{u}_k^+(\boldsymbol{x}) - \tilde{u}_k^-(\boldsymbol{x})$ are displacement discontinuities on the crack surface Γ_c, u_k^+ and u_k^- are displacements on the upper and lower crack surfaces respectively, $\tilde{U}_{ij}(\boldsymbol{X}', \boldsymbol{x}, s)$ and $\tilde{T}_{ij}(\boldsymbol{X}', \boldsymbol{x}, s)$ are the Laplace transformed fundamental solutions of elastodynamic displacement and traction respectively

and the functions $\tilde{U}_{kij}(\boldsymbol{X}', \boldsymbol{x}, s)$ and $\tilde{T}_{kij}(\boldsymbol{X}', \boldsymbol{x}, s)$ contain derivatives of the fundamental solutions (see Wen *et al.*, 1998).

The displacement boundary integral equation for the point on the external boundary Γ_e can be obtained from Eq. (6) by considering the limit as the domain point $\boldsymbol{X}' \to \boldsymbol{x}'$ on the boundary. The same procedure as illustrated in Aliabadi and Rooke (1991) can be used to obtain the displacement boundary integral in the Laplace domain as

$$c_{ij}(\boldsymbol{x}')\tilde{u}_j(\boldsymbol{x}') = \int_{\Gamma_e} \tilde{U}_{ij}(\boldsymbol{x}', \boldsymbol{x}, s)\tilde{t}_j(\boldsymbol{x})d\Gamma(\boldsymbol{x}) - \oint\!\!\!\!\!\!-_{\Gamma_e} \tilde{T}_{ij}(\boldsymbol{x}', \boldsymbol{x}, s)\tilde{u}_j(\boldsymbol{x})d\Gamma(\boldsymbol{x}) - \int_{\Gamma_c} \tilde{T}_{ij}(\boldsymbol{x}', \boldsymbol{x}, s)\Delta\tilde{u}_j(\boldsymbol{x})d\Gamma(\boldsymbol{x}) \quad (8)$$

where $\int$ denotes a Cauchy principal–value integral and $c_{ij}(\boldsymbol{x}')$ is a function of the geometric shape at the boundary point $\boldsymbol{x}'$; $c_{ij}(\boldsymbol{x}')=\delta_{ij}/2$ for a point on a smooth boundary. The traction can be written, on the crack surface, as

$$\tilde{t}_j(\boldsymbol{x}') = n_i \int_{\Gamma_e} \tilde{U}_{kij}(\boldsymbol{x}', \boldsymbol{x}, s)\tilde{t}_k(\boldsymbol{x})d\Gamma(\boldsymbol{x}) - n_i \int_{\Gamma_e} \tilde{T}_{kij}(\boldsymbol{x}', \boldsymbol{x}, s)\tilde{u}_k(\boldsymbol{x})d\Gamma(\boldsymbol{x}) - n_i \oint\!\!\!\!\!\!-_{\Gamma_c} \tilde{T}_{kij}(\boldsymbol{x}', \boldsymbol{x}, s)\Delta\tilde{u}_k(\boldsymbol{x})d\Gamma(\boldsymbol{x}) \quad (9)$$

where $n_i(\boldsymbol{x}')$ is the normal unit vector on the boundary and $\int$ denotes a Hadamard principal–value integral (1923). By solving these Eqs. (8) and (9), the displacements and tractions on the external boundary Γ_e and discontinuity displacements on the crack surface Γ_c can be obtained numerically with given boundary conditions for linear elastodynamic problem. The stress intensity factors in the Laplace transform domain is evaluated by discontinuity displacements at the nodes in front of the crack tip directly as shown in Wen and Wang (1991).

III. FRICTIONAL CONTACT ANALYSIS

Consider a body with a flat crack subjected to a dynamic load $F(\boldsymbol{x}, t)\boldsymbol{n}'$, where $\boldsymbol{n}'$ is unit vector of load, the local coordinate system (x_1, x_2, x_3) is established on the crack as shown in Fig. 1(a). The axis x_2 is along the normal of crack ($\boldsymbol{n}_2=\boldsymbol{n}$), $\boldsymbol{n}_1$, $\boldsymbol{n}_2$ and $\boldsymbol{n}'$ are in the same plane, i.e. $\boldsymbol{n}' \cdot (\boldsymbol{n}_1 \times \boldsymbol{n}_2)=0$. The contact between two crack surfaces is caused by an external load.

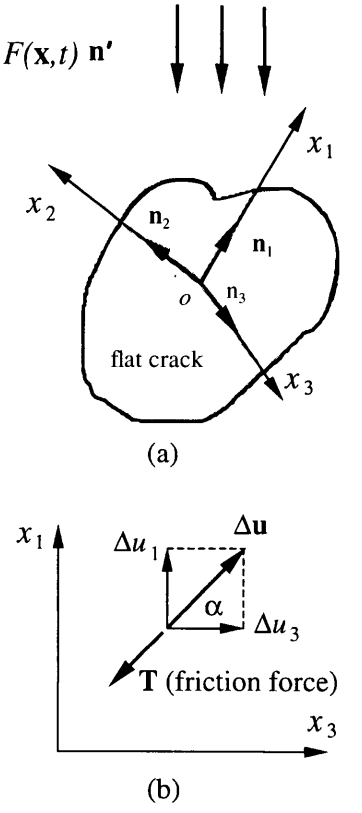

Fig. 1. Flat crack and local co-ordinate.

1. Mode of Contact

Under the external dynamic load $F(\boldsymbol{x}, t)\boldsymbol{n}'$, the contact will occur on the crack surfaces. There are three modes to describe the contact between crack surfaces: separation mode, slip mode and stick mode. The boundary values on the crack surface should satisfy the contact conditions for different modes in the time domain. The different contact conditions can be written as:

(i) Separation mode:

$$t_1(t)=0;\ t_2(t)=0;\ t_3(t)=0 \text{ and } \Delta u_2 \geq 0, \quad (10)$$

with unknowns $\Delta u_1(t)$, $\Delta u_2(t)$ and $\Delta u_3(t)$.

(ii) Slip mode:

$$\Delta u_2(t)=0;\quad t_1(t)=-\mu t_2(t)\frac{\Delta u_1}{\sqrt{\Delta u_1^2+\Delta u_3^2}}$$

and

$$t_3(t)=-\mu t_2(t)\frac{\Delta u_3}{\sqrt{\Delta u_1^2+\Delta u_3^2}}, \quad (11)$$

with unknowns $t_2(t)$ (≤ 0), $\Delta u_1(t)(\neq 0)$ and $\Delta u_3(t)(\neq 0)$ [see Fig. 1(b)].

(iii) Stick mode:

$$\Delta u_1(t)=0;\ \Delta u_2(t)=0;\ \Delta u_3(t)=0$$

and

$$\sqrt{t_1(t)^2+t_3(t)^2} \le -\mu t_2(t), \tag{12}$$

with unknowns $t_1(t)$, $t_2(t)$ (≤ 0) and $t_3(t)$. The term μ denotes the coefficient of friction.

As the contact region depends on the magnitude of dynamic load and time and the relationship between contact pressure and the friction is nonlinear in the stick region, it is difficult to solve the problem in the Laplace transform domain. Wen, *et al.* (1995) developed a successive technique to analyse the dynamic frictionless contact for symmetrical crack problems. Because the crack is flat and the ratio $|\Delta u_3|/|\Delta u_1|$ is very small for frictionless contact problems, this highly nonlinear contact problem can be simplified with two assumptions:

- The contact region is initiated in the slip mode.
- The friction $t_3(t)$ is zero.

Under these two assumptions, this nonlinear problem can be simplified to linear problem and the boundary condition on the crack surface can be written as

$$\Delta u_2(t)=0;\ t_1(t)=\mu t_2(t) \text{ and } t_3(t)=0, \tag{13}$$

and in the Laplace transform domain, they become

$$\Delta \tilde{u}_2(s)=0;\ \ \tilde{t}_1(s)=\mu \tilde{t}_2(s) \text{ and } \tilde{t}_3(s)=0. \tag{14}$$

with unknowns $\Delta\tilde{u}_1(s)$, $\Delta\tilde{u}_3(s)$ and $\tilde{t}_2(s)$ (contact pressure). After the analysis, the contact tractions and displacements are checked and the above conditions are corrected accordingly.

2.Traction Boundary Integral Equation

Consider the normal $n_1=0$, $n_2=1$ and $n_3=0$ in the local coordinate, substituting traction Eq. (9) into contact condition Eq. (14) gives the following equations for the collocation point on the crack surface

$$\Delta\tilde{u}_2=0; \tag{15}$$

$$\int_{\Gamma_e} [\tilde{U}_{k21}(\boldsymbol{x}',\boldsymbol{x},s)-\mu\tilde{U}_{k22}(\boldsymbol{x}',\boldsymbol{x},s)]\tilde{t}_k(\boldsymbol{x})d\Gamma(\boldsymbol{x})$$

$$-\int_{\Gamma_e} [\tilde{T}_{k21}(\boldsymbol{x}',\boldsymbol{x},s)-\mu\tilde{T}_{k22}(\boldsymbol{x}',\boldsymbol{x},s)]\tilde{u}_k(\boldsymbol{x})d\Gamma(\boldsymbol{x})$$

$$-\oint\!\!\!\!\!\!=_{\Gamma_c} [\tilde{T}_{k21}(\boldsymbol{x}',\boldsymbol{x},s)-\mu\tilde{T}_{k22}(\boldsymbol{x}',\boldsymbol{x},s)]\Delta\tilde{u}_k(\boldsymbol{x})d\Gamma(\boldsymbol{x})=0 \tag{16}$$

and

$$\int_{\Gamma_e} \tilde{U}_{k23}(\boldsymbol{x}',\boldsymbol{x},s)\tilde{t}_k(\boldsymbol{x})d\Gamma(\boldsymbol{x})-\int_{\Gamma_e} \tilde{T}_{k23}(\boldsymbol{x}',\boldsymbol{x},s)\tilde{u}_k(\boldsymbol{x})d\Gamma(\boldsymbol{x})$$

$$-\oint\!\!\!\!\!\!=_{\Gamma_c} \tilde{T}_{k23}(\boldsymbol{x}',\boldsymbol{x},s)\Delta\tilde{u}_k(\boldsymbol{x})d\Gamma(\boldsymbol{x})=0. \tag{17}$$

The numerical results for frictional contact problems can be obtained approximately by solving boundary integral Eq. (8)(9)(16) and (17) with external and crack boundary conditions given by Eqs. (4)(5) and (15).

3. Numerical Technique for Boundary Integral Equations

For an embedded crack problem, the displacement and traction boundary integral Eqs. (8),(9),(16) and (17) are discretized with two different types of elements, quadratic continuous elements on the external boundary Γ_e and quadratic discontinuous elements on the crack surfaces Γ_c. The displacement or discontinuity displacement and traction on the element n are approximated as

$$\tilde{u}_i^n(\xi,\eta)=\sum_{\alpha=1}^{8} N^\alpha(\xi,\eta)\tilde{u}_i^{n\alpha} \tag{18}$$

or

$$\Delta\tilde{u}_i^n(\xi,\eta)=\sum_{\alpha=1}^{8} M^\alpha(\xi,\eta)\tilde{u}_i^{n\alpha} \tag{19}$$

and

$$\tilde{t}_i^n(\xi,\eta)=\sum_{\alpha=1}^{8} N^\alpha(\xi,\eta)\tilde{t}_i^{n\alpha} \tag{20}$$

where $\tilde{u}_i^{n\alpha}$, $\Delta\tilde{u}_i^{n\alpha}$ and $\tilde{t}_i^{n\alpha}$ are displacement or discontinuity displacement and traction values at the node α, $N^\alpha(\xi,\eta)$ and $M^\alpha(\xi,\eta)$ are shape functions which depend on the type of elements. The use of these approximations enables the displacement and traction boundary integral Eqs. to be discretized, in matrix form, as

$$\boldsymbol{H}\begin{Bmatrix}\tilde{\boldsymbol{u}}\\ \Delta\tilde{\boldsymbol{u}}\end{Bmatrix}=\boldsymbol{G}\{\tilde{\boldsymbol{t}}\} \tag{21}$$

where

$$\boldsymbol{H}=\begin{bmatrix}\boldsymbol{H}_{ee}\ \boldsymbol{H}_{ec}\\ \boldsymbol{H}_{ce}\ \boldsymbol{H}_{cc}\end{bmatrix},\quad \boldsymbol{G}=\begin{bmatrix}\boldsymbol{G}_{ee}\\ \boldsymbol{G}_{ce}\end{bmatrix},$$

matrix $\boldsymbol{H}$ contains integrals involving $\tilde{T}_{ij}$ and $\tilde{T}_{kij}$, and matrix $\boldsymbol{G}$ contains integrals involving $\tilde{U}_{ij}$ and $\tilde{U}_{kij}$ respectively. The vectors $\tilde{\boldsymbol{u}}$, $\Delta\tilde{\boldsymbol{u}}$ and $\tilde{\boldsymbol{t}}$ consist of all nodal displacement, discontinuity displacement and

traction components on the boundary. After application of the boundary conditions and rearrangement of the columns in matrices $\boldsymbol{H}$ and $\boldsymbol{G}$ all the unknowns are passed to a vector $\boldsymbol{x}$ on the left side, leading to the following linear system of equations

$$\{A\}\{x\}=\{y\} \tag{22}$$

where y is the vector for known components. All boundary values on nodal points of $\tilde{u}_k$, $\Delta\tilde{u}_k$ and $\tilde{t}_k$ can be obtained after solving Eq. (22). Stress intensity factors at crack tips can be obtained from displacement discontinuity (COD) directly as illustrated in Mi and Aliabadi (1992). Contact pressure can be determined from following equation for flat crack:

$$\tilde{t}_2(x')=\int_{\Gamma_e}\tilde{U}_{k22}(x',x,s)\tilde{t}_k(x)d\Gamma(x) - \int_{\Gamma_e}\tilde{T}_{k22}(x',x,s)\tilde{u}_k(x)d\Gamma(x). \tag{23}$$

4. Durbin's Inversion Method

The time–dependent values of any of the transformed variables must be obtained by an inverse transform. The calculation formula used is as follows, Durbin (1974)

$$f(t)=2\frac{e^{ct}}{T}[-\frac{1}{2}\Re\{\tilde{f}(c)\} + \sum_{k=0}^{L}(\Re\tilde{f}(c+i\frac{2k\pi}{T})\cos\frac{2k\pi t}{T} - \Im\tilde{f}(c+i\frac{2k\pi}{T})\sin\frac{2k\pi t}{T})] \tag{24}$$

where $\tilde{f}(s_k)$ stands for the value in Laplace space at the sample point

$$s_k=c+2k\pi i/T \quad \text{and} \quad i=\sqrt{-1}\,.$$

The sample points are chosen for k=0, 1, ..., L. Good results have been obtained for cT=5 and T/t_0=20, where t_0 is unit time, for instance $t_0=c_1t/h$ for rectangular bar in the following example [h is half of height of the bar (Wen *et al.*, 1998)].

To check if these two assumptions are correct, the time dependent contact pressure $p(t)=-t_2(t)$ and discontinuity displacement $\Delta u_1(t)$ and $\Delta u_3(t)$ can be plotted. When $p(t)<0$ (separation mode) or $\Delta u_1(t')=0$ and $\Delta u_3(t')=0$ (stick mode) occurs in contact region, successive modification technique (Wen *et al.*, 1995) should be used to obtain more accurate solutions.

IV. NUMERICAL EXAMPLE

We consider a square bar with a slant circular crack loaded by a uniform pressure stress $F(x, t)=p_0H(t)$ at the top of the bar as shown in Fig. 2. The bottom of the bar is fixed [$u_k(t)=0$, k=1, 2, 3]. The width of the bar is $2w$, the height $2h$, the radius of circular crack a with $h=2w$, $a=0.5w$ and the slant angle β=45°. The Poisson's ratio ν=0.3, and the shear wave velocity $c_2=0.5345c_1$. There are 40 continuous elements used on the external boundary with 122 nodes and 20 discontinuity elements on the crack with 160 nodes as same as Mi and Aliabadi (1992).

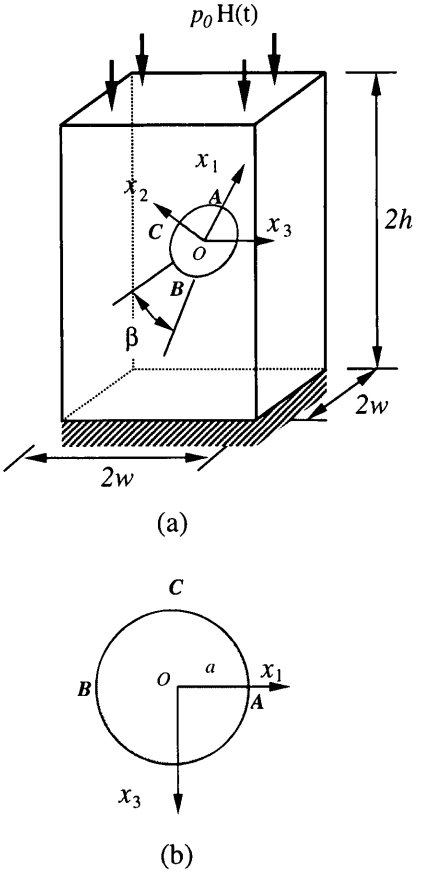

Fig. 2. Cracked body and local co-ordinate on the crack surface.

It is well known that the dynamic stress intensity factors are influenced by elastic waves which start from traction boundary (Lin and Ballman, 1993; Wen *et al.*, 1996). Fig. 3 shows the dynamic shear stresses $\tau_1(t)$ at points A and B in the local coordinate system without the crack in the body under load $p_0H(t)$, where the number of Laplace transform parameter L is chosen to be 95. There are ten main elasticity waves as listed in Table 1 to make shear stress curves change sharply. The first wave (I_1) arrived at point A is a P–wave leaving from the top at normalized time $\bar{t}=c_1t/h$=0.823 (see Fig. 4). Since the boundary of bar is free, a P–wave and S–wave will be produced there to satisfy the free boundary condition. So the second wave should be the P–wave starting from the corner

Table 1. Elasticity waves at point A

number k	speed	time to arrive $\bar{\tau}_k$	number k	speeds	time to arrive $\bar{\tau}_k$
1	c_1	$0.823(I_1)$	6	c_1+c_2	$2.334(I_6)$
2	c_1	$0.884(I_2)$	7	c_1+c_2	$2.614(I_7)$
3	c_2	$1.334(I_3)$	8	c_1+c_2	$2.894(I_8)$
4	c_2	$1.614(I_4)$	9	c_1+c_2	$3.688(I_9)$
5	c_2	$1.894(I_5)$	10	c_1+c_2	$4.284(I_{10})$

Table 2. Elasticity waves at point B

number k	speed	time to arrive $\bar{\tau}_k$	number k	speeds	time to arrive $\bar{\tau}_k$
1	c_1	$1.177(I_1)$	6	c_1+c_2	$2.688(I_6)$
2	c_1	$1.221(I_2)$	7	c_1+c_2	$2.968(I_7)$
3	c_2	$1.688(I_3)$	8	c_1+c_2	$3.248(I_8)$
4	c_2	$1.968(I_4)$	9	c_1+c_2	$3.334(I_9)$
5	c_2	$2.248(I_5)$	10	c_1+c_2	$3.894(I_{10})$

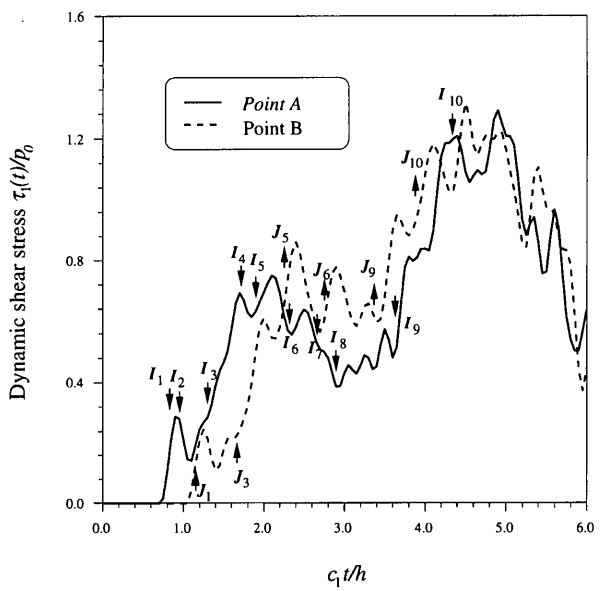

Fig. 3. Dynamic shear stress at point A and B.

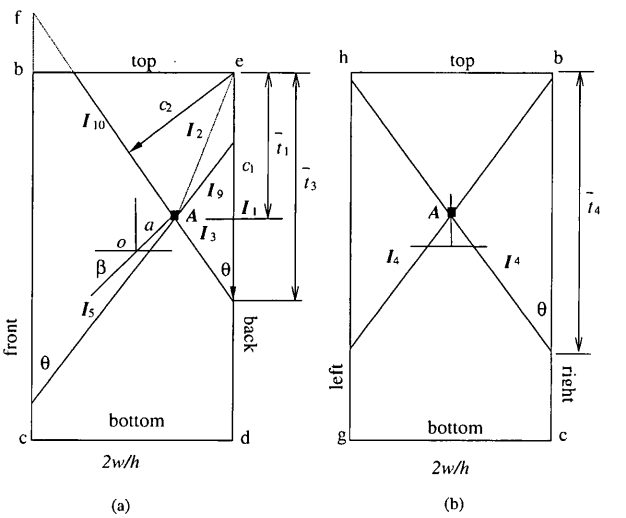

Fig. 4. Elasticity waves and their paths to point A without crack.

e (wave I_2) at $\bar{t}_2 = \overline{eA} = 0.884$. Waves 3, 4 and 5 ($I_3$, I_4, I_5) should be the S-waves coming from the four free boundaries (front, back, left and right) as shown in Fig. 4 (see Lin and Ballman, 1993 for two dimensional problem), where $\theta = \sin^{-1}(c_2/c_1)$. Wave 6 ($I_6$) should be produced by the elastic waves traveling from the front boundary (b) to the back (e) at speed c_1 and then travelling at shear waves speed to A, the time $\bar{t}_6 = \overline{be} + \bar{t}_3 = 2.334$. The waves 7 ($I_7$) and 8 ($I_8$) are similar to wave 6, $\bar{t}_7 = \overline{hb} + \bar{t}_4$ and $\bar{t}_8 = \overline{eb} + \bar{t}_5$. Waves 9 ($I_9$) and 10 ($I_{10}$) are caused by the shear waves reflected from to point A. It is clear that $t_9 = 2 + 0.177 + 0.323\text{ctg}\theta = 3.688$ and $t_{10} = 2 + 0.177 + 0.617\text{ctg}\theta = 4.248$. In addition there should be more elastic waves reflected from the boundaries, such as the waves from the junction lines. The shear stress at point B can be explained in the same way. The arrival times of elastic wave to point B starting from the top or being reflected from the boundary are listed in Table 2. The waves are labelled as J_k.

The dynamic stress intensity factors $K_{II}^A(t)$, $K_{II}^B(t)$ at crack tips A and B and $K_{III}^C(t)$ at point C are shown in Figs. 5, 6 and 7 for friction coefficient $\mu = 0$, 0.1 and 0.2, where $K^0 = p_0\sqrt{2a/\pi}$ and the number of Laplace transform parameter L is chosen to be 50. It is evident that the curves of dynamic stress intensity factor (at point A or point B) have the similar configuration of shear stress (at point A or point B) as shown in Fig. 3. The influence on dynamic stress intensity factors by waves 1, 3, 5, 6, 8, 9 and 10 are very significant because the stress intensity factors change greatly at these times $\bar{t}_k$. In addition, the stress intensity factors must be influenced by P–waves and surface waves travelling along the crack surface

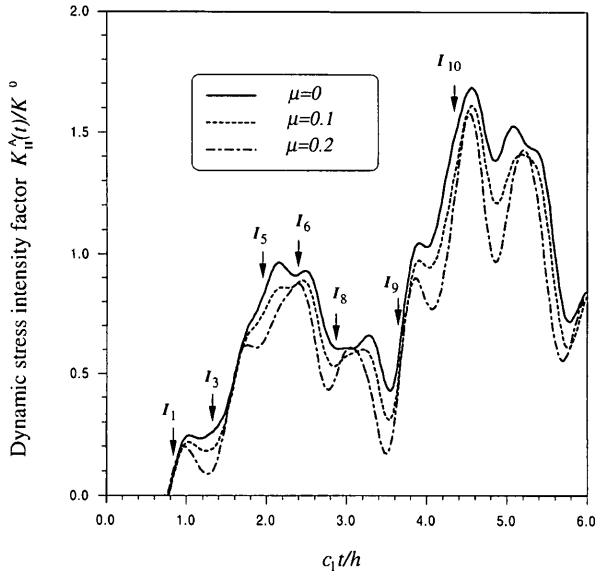

Fig. 5. Dynamic stress intensity factors at point A for different friction coefficient.

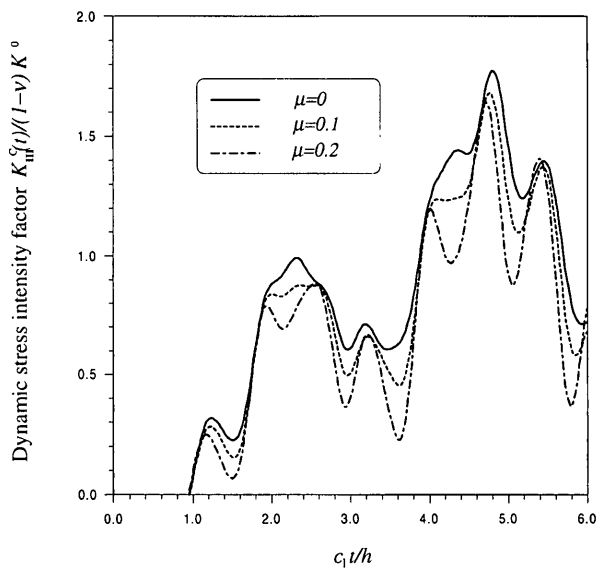

Fig. 7. Dynamic stress intensity factors at point C for different friction coefficient.

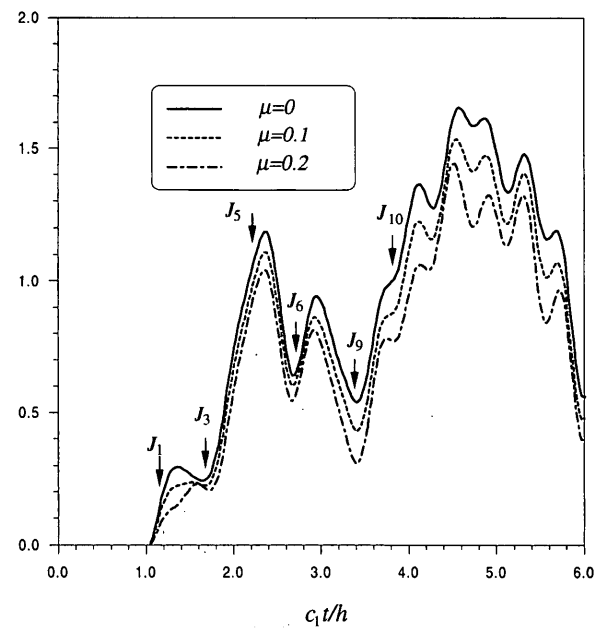

Fig. 6. Dynamic stress intensity factors at point B for different friction coefficient.

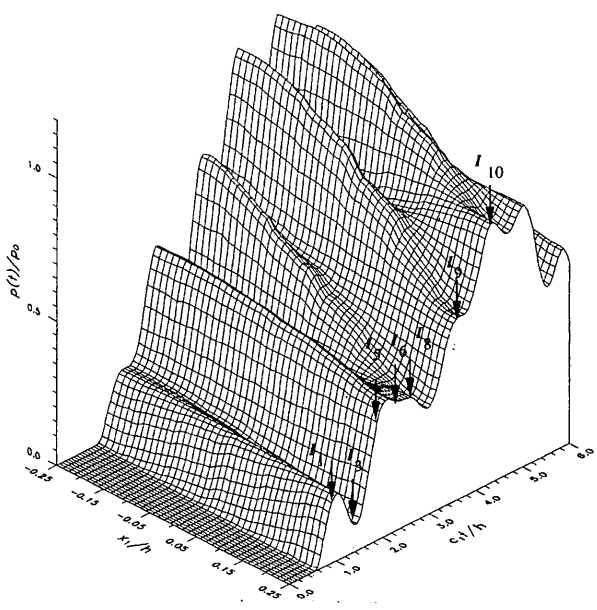

Fig. 8. Contact pressure $p(t)/p_0$ between two point A and B (3D plot).

as illustrated in Lin and ballman (1993); Wen *et al.* (1996). As the accuracy of numerical method, those influence can not be seen here clearly.

To check the contact pressure in contact region, the pressure $p(t)/p_0$ when friction coefficient μ=0 along the line $\overline{AB}$ is shown in Figs. 8 and 9 (there is very little difference between the results for μ=0 and μ=0.2). From Fig. 8, it is seen that the contact (no separation) occurs on the whole crack surface as $p(t)>0$ when $0\leq \overline{t} \leq 6$. Since the displacement discontinuity $\Delta u_1(t)$ and $\Delta u_3(t)$ do not change their signs and the pressure $p(t)$ are larger than zero in the whole contact region when $(0\leq \overline{t} \leq 6)$, the assumptions (1) and (2) are correct for this example.

V. CONCLUSION

The flat crack closure frictional contact problem is analysed in this paper. Two assumptions allow the highly nonlinear elasodynamic problem to be transformed to a linear problem in the Laplace transformed domain. Boundary integral equations are

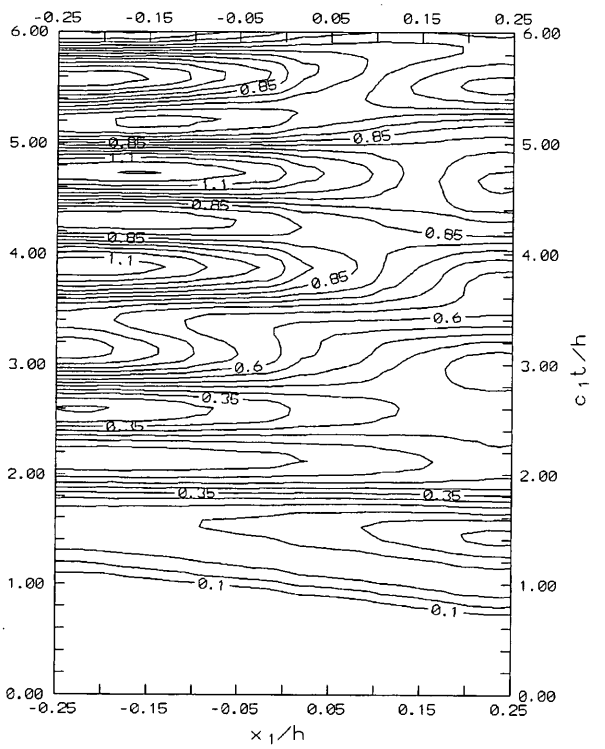

Fig. 9. Contact pressure $p(t)/p_0$ (contour plot).

given for flat crack under simple dynamic load and solved numerically by quadratic elements. Durbin's inversion technique is used to obtain the solutions in the time domain. By considering of the dynamic shear stresses without crack under the same load, the influences on dynamic stress intensity factors by elasticity waves are discussed.

ACKNOWLEDGEMENT

This work has been carried out with the support of the Ministry of Defence, Defence Evaluation and Research Agency, FARNBOROUGH, Hants, U.K.

REFERENCES

1. Andersson, T., 1984, "The Boundary Element Method Applied to Two–Dimensional Contact Problem with Friction," *Boundary Element Method*, Springer Publication, Berlin, pp. 409-427.
2. Aliabadi, M.H., and Rooke, D.P., 1991, *Numerical Fracture Mechanics*, Computational Mechanics Publications and Kluwer Academic Publishers.
3. Balas, J., Sladek, J., and Sladek, V., 1989, *Stress Analysis by Boundary Element Method*, Elsevier.
4. Chan, C.H. and Tuba, I.S., 1971, "A Finite Element Method for Contact Problems of Solid Bodies: I. Theory and validation," *International Journal of Mechanics Science*, Vol. 13, pp. 615-625.
5. Chan, C.H., and Tuba, I.S., 1971, "A Finite Element Method for Contact Problems of Solid Bodies: Application to Turbine Blade Fastenings," *International Journal of Mechanics Science*, Vol. 13, pp. 627-639.
6. Chen J.T., and Hong H.K, 1999, "Review of Dual Boundary Element Methods with Emphasis on Hypersingular Integrals and Divergent Series", *Applied Mechanics Review*, Vol. **52**(1), pp. 17-33.
7. Durbin, F., 1974, "Numerical Inversion of Laplace Transforms: an Efficient Improvement to Dubner and Abate's method," *Computer Journal*, Vol. 17, No. 4, pp. 371-376.
8. Hadamard, J., 1923, *Lectures on Cauchy's Problem in Linear Partial Differential Equations*, Yale University Press, New Haven.
9. Hertz, H., 1986, *On the contact of elastic solid*, Translated by Johnes, D. E., Macmillan and Co. Ltd., London.
10. Hong H.K., and Chen J.T., 1988, "Derivation of Integral Equations in Elasticity", *Journal of Engineering Mechanics, ASCE* **114**, pp. 1028-1044.
11. Lin, X., and Ballman, J., 1993, "Re–consideration of Chen's Problem by Finite Difference Method," *Engineering Fraction Mechanics*, Vol. 44, pp. 735-739.
12. Mi, Y., and Aliabadi, M.H., 1992, "Dual Boundary Element for Three–Dimensional Fracture Mechanics Analysis," *Engineering Analysis with Boundary Elements*, Vol. 10, No. 2, pp. 161-171.
13. Man. K., Aliabadi, M.H., and Rooke, D.P., 1993, "Analysis of Contact Friction Using the Boundary Element Method," *Computational Methods in Contact Mechanics*, Edited by M. H. Aliabadi and C. A. Brebbia, Computational Mechanics Publications.
14. Wen, P.H. Aliabadi, M.H., and Rooke, D.P., 1995, "An Approximate Analysis of Dynamic Contact between Crack Surfaces," *Engineering Analysis with Boundary Element*, Vol. 16, pp. 41-46.
15. Wen, P.H. Aliabadi, M.H., and Rooke, D.P., 1996, "The Influence of Elastic Waves on Dynamic Stress Intensity Factors (Two–dimensional Problems)," *Archive of Applied Mechanics*, Vol. 66, pp. 326-335.
16. Wen, P.H. Aliabadi, M.H., and Rooke, D.P., 1996, "The Influence of Elastic Waves on Dynamic Stress Intensity Factors (Three–dimensional Problems), *Archive of Applied Mechanics*, Vol. 66, pp. 385-394.
17. Wen, P.H. Aliabadi, M.H., and Rooke, D.P.,

1998, "Cracks in Three–dimensions: a Dynamic dual Boundary Element Analysis," *Computer Methanics Applied Mechanics Engineering*, Vol. 167, pp. 139-151.
18. Wilson, E.A., and Parsons, B., 1970, "Finite Element Analysis of Elastic Contact Problems Using Differential Displacements," *International Journal of Numerical Mechanics Engineering*, Vol. 2, pp. 384-395.
19. Wen, P.H., and Wang Y., 1991, "The Calculation of SIF Considering the Effects of Arc Crack Surface Contact and Friction Under Uniaxial Tension and Pressure," *Engineering Fracture Mechanics*, Vol. 39,Vol. 4, pp. 651-660.

Discussions of this paper may appear in the discussion section of a future issue. All discussions should be submitted to the Editor-in-Chief.

Manuscript Received: May 04, 1999
Revision Received: July 10, 1999
and Accepted: Aug. 15, 1999

三維結構物於動態的裂縫摩擦接觸分析

文丕華　M.H. Aliabadi

倫敦大學瑪麗皇后和西域學院工程系

A. Young

杭特斯 DERA 結構材料中心

摘　要

在本文中我們發展出對偶邊界元素的架構來探討當受到動磨擦負載時裂縫表面接觸的問題。藉由三個假設我們可將三維非線性動力問題處理成線性問題。而對偶邊界積分方程的狀態變量爲拉氏（Laplace）轉換域的外圍邊界位移，外圍邊界曳引力與裂縫面位移不連續量。並且採用杜賓（Durbin）的拉氏反轉換法及藉由裂縫開口的位移來決定應力強度因子。本文並探討一長方形含有一個傾斜圓形裂縫棒受階梯負載時的反應。同時詳細的分析在不同彈性波對應力強度因子 $K_{II}(t)$及 $K_{III}(t)$的影響。

關鍵詞：邊界元素法，接觸力學，斷裂力學，動應力強度。